JOURNAL OF COLLOID AND INTERFACE SCIENCE **204,** 151–156 (1998)
ARTICLE NO. CS985515

Characterization of Structural and Surface Properties of Activated Carbon Fibers

Zuojiang Li, Michal Kruk, Mietek Jaroniec,[1] and Seung-Kon Ryu

Department of Chemistry, Kent State University, Kent, Ohio 44242; and Department of Chemical Engineering, Chungnam National University, Taejon, Korea

Received December 23, 1997; accepted March 5, 1998

Nitrogen adsorption isotherms on activated carbon fibers (ACFs) were measured at 77.3 K in the relative pressure range from 10^{-7} to 0.995. The low relative pressure data are examined in detail in order to characterize the microporosity and the surface heterogeneity of the samples studied. The pore structure of ACFs was studied by using the α_s plot and DFT methods. Adsorption potential and adsorption energy distributions were also calculated. The results showed that ACFs are highly microporous and in some cases contain small mesopores (2–4 nm). ACFs exhibit a significant structural and energetic heterogeneity.

Key Words: **adsorption; activated carbon fiber; microporosity.**

INTRODUCTION

Porous carbons are widely used in separation, purification and catalytic processes due to their excellent adsorption properties (1, 2). During the past ten years, activated carbon fibers have attracted considerable attention because of their high adsorption rates and capacities, ease of synthesis in various forms, and wide applicability (3–13). In spite of the fact that porous carbons have been extensively studied in the past, there is still a need to improve and/or develop simple and convenient methods of their characterization. The assessment of microporosity and micropore size distributions is particularly challenging. Gas adsorption methods have been usually applied for these purposes. However, the conventional adsorption methods to calculate pore size distributions, i.e. those based on the Kelvin equation (14) are not applicable for micropores. Therefore, other characterization methods have been introduced, including the Dubinin–Radushkevich (DR) (15), the Dubinin–Astakhov (DA) (16), the comparative plot (t plot, α_s plot) (17–21), MP (22), and the Horvath–Kawazoe (HK) methods (23). All of these approaches have their limitations and the results obtained using these methods often differ from one another. The DR and DA equations are suitable to describe gradually increasing and S-shaped (in a logarithmic scale) adsorption isotherms, rarely observed for microporous carbons in the case of nitrogen adsorption isotherms, which often exhibit quite abrupt increase in the adsorbed amount at very low pressures and then level off (24, 25). The HK method is expected to be suitable only for porous carbons with predominant micropores of width below ca. 1 nm. The HK approach is based on the condensation approximation (20) and assumes one-step filling of micropores, which is grossly inaccurate for wider micropores, where there are distinct stages of monolayer formation and subsequent condensation inside the pore (14, 26, 28). Consequently, the HK method attributes the monolayer capacity of pores wider than ca. 1 nm to the volume of nonexisting micropores of the size ca. 0.6 nm (when original parameters from Ref. (23) are used) (24). The comparative plot methods are very convenient in obtaining the micropore volume and qualitative information about the micropore size (17, 29, 30), but they are not suitable for evaluation of micropore size distributions. In the MP method (22), the statistical thickness is used in calculations, which is equivalent to an assumption that the course of adsorption on the surface of pores is the same as that on the flat surface of a macroporous reference adsorbent. Consequently, the enhancement of adsorption in micropores due to their small dimensions (14–16, 26, 28) is neglected, which is expected to lead to a significant underestimation of the micropore size and makes the method inherently unsuitable for micropore analysis. It can be concluded that most of the procedures currently used to assess microporosity are subject to severe limitations in their applicability.

To overcome these difficulties, new methods have been developed based on the concept of the integral equation for overall adsorption and employing advanced modeling of local adsorption isotherms using the nonlocal density functional theory or computer simulation methods (14, 26, 28, 31, 32). These approaches are capable of providing a good fit to experimental adsorption data and their application is not limited to the micropore size range (14, 28, 31).

In the current study, nitrogen adsorption isotherms were

[1] To whom correspondence should be addressed. E-mail: Jaroniec@scorpio.kent.edu.

0021-9797/98 $25.00

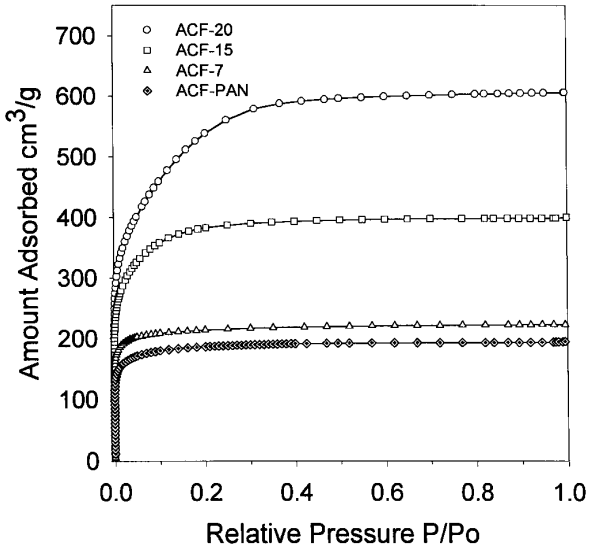

FIG. 1. Nitrogen adsorption isotherms on activated carbon fibers, shown in the linear scale.

measured in a wide range of relative pressures (ca. 10^{-7}–0.995) for several activated carbon fiber samples, and the adsorption data were used for a detailed characterization of their porous structures. The pore size distributions were calculated by using advanced DFT software (31). The comparative plots, adsorption potential distributions, and adsorption energy distributions were also examined and shown to provide useful information about the structural and surface properties of activated carbon fibers. It was concluded that when adsorption data are acquired starting from very low relative pressures, proper calculation methods allow one to gain thorough insight into microporous structures of ACFs.

MATERIALS AND METHODS

1. Samples

The ACF-7, ACF-15, and ACF-20 samples were coal tar-based activated carbon fibers from Osaka Gas Co. Ltd, Japan. Their application as catalyst supports was studied elsewhere (33). The manufacturer's notation of the samples indicates their approximate specific surface area expressed in hundreds of square meters per gram (e.g., 2000 m^2/g for ACF-20). ACF-PAN was a polyacrynitrile-based, steam-activated sample from Institute of Coal Chemistry, Chinese Academy of Sciences.

2. Measurements

Nitrogen adsorption measurements were performed at 77.3 K on a volumetric adsorption analyzer ASAP 2010 (Micromeritics, Norcross, GA), which allows us to measure the adsorption isotherms starting from very low relative pressures (10^{-7}–10^{-6}). All samples were degassed at 523 K in vacuum for 3 h before measurement.

3. Calculation Methods

BET specific surface areas of the samples studied were obtained through the standard BET (17) method in the relative pressure range from 0.04 to 0.14. The total pore volume was calculated from the amount adsorbed at relative pressure 0.995. The micropore volume and the external surface area were obtained from a high-resolution α_s plot using a non-graphitized carbon black as a reference adsorbent (25). The pore size distributions were calculated by density functional theory (DFT) software developed by the Micromeritics Company. Further details of this method can be found elsewhere (31).

The differential adsorption potential distributions were calculated by the numerical differentiation of adsorption isotherm $v(A)$ with respect to the adsorption potential A. The adsorption potential is defined to be equal to the change in the Gibbs free energy of adsorption, $A = RT\ln(p_o/p)$, where R is the universal gas constant, T is the absolute temperature, p is the equilibrium gas pressure, and p_0 is the saturated vapor pressure.

The adsorption energy distributions were obtained from submonolayer data using the Fowler–Guggenheim kernel (localized monolayer adsorption with lateral interaction) in the integral equation of adsorption (34). The interaction parameter $wz/k_B = 190$ K was adopted in the calculation (35). The choice of the local adsorption isotherm model and the parameters was discussed in Ref. (27).

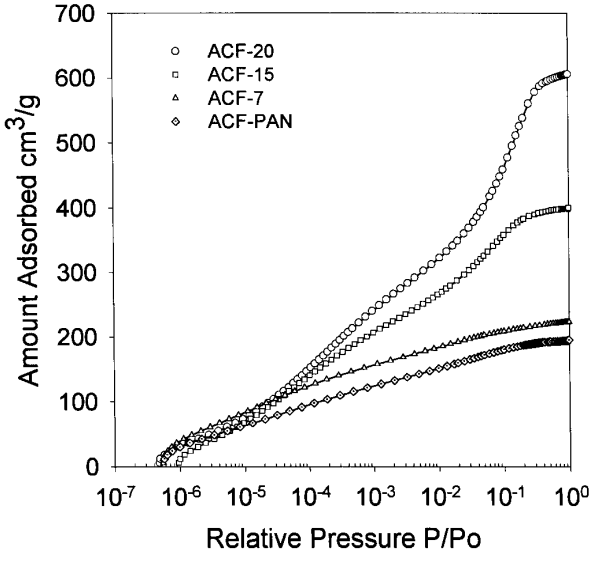

FIG. 2. Nitrogen adsorption isotherms of activated carbon fibers, shown in the logarithmic scale.

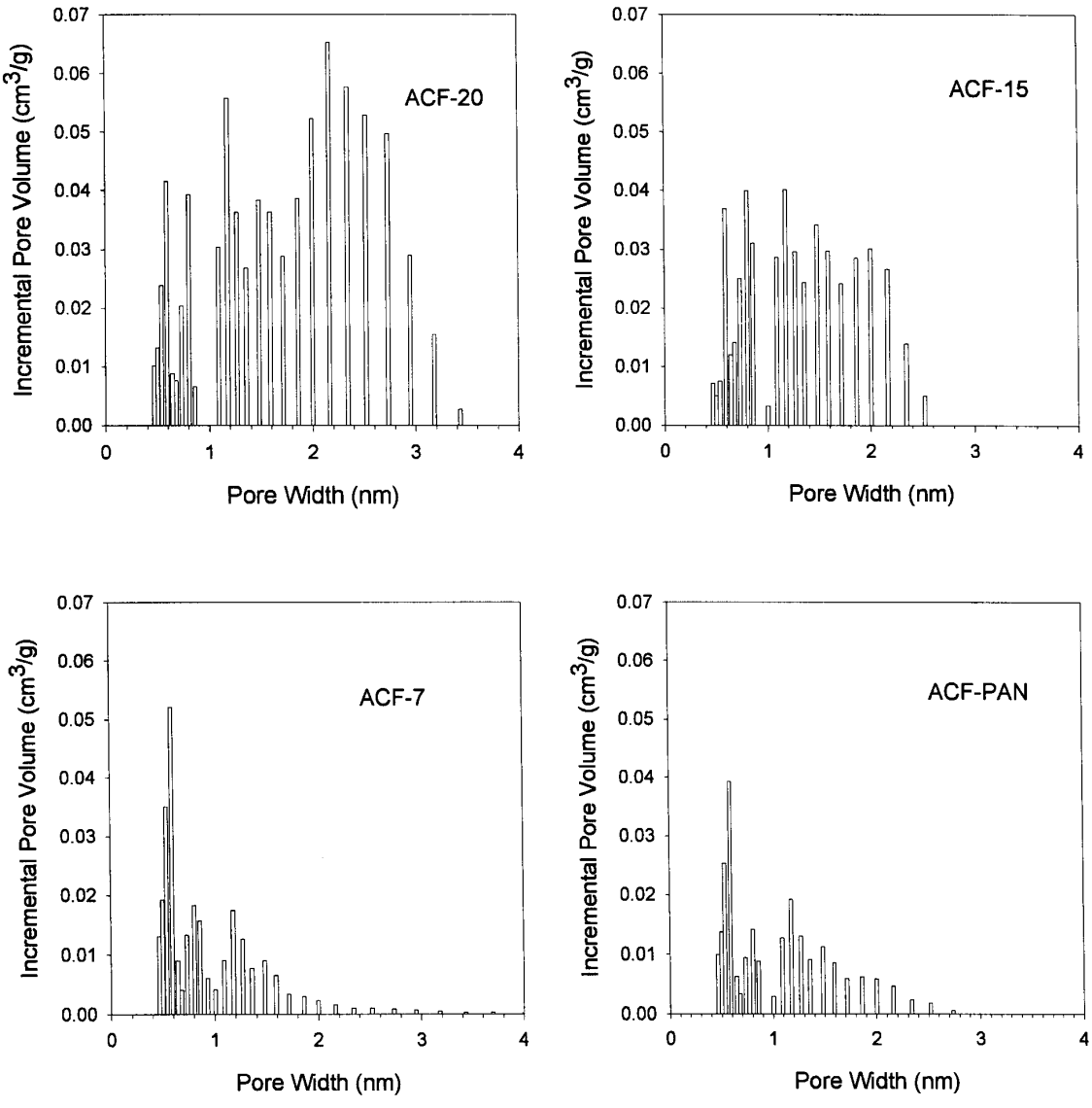

FIG. 3. Pore size distributions for ACFs calculated using the DFT software.

RESULTS AND DISCUSSION

1. Adsorption Isotherms

Nitrogen adsorption isotherms for the ACF samples studied are shown in the linear scale in Fig. 1. All isotherms are of type I according to the IUPAC classification (17, 18), which shows the domination of micropores in the pore structure. However, there are some differences between ACF-20, ACF-15, and the other two samples. The former show a gradual adsorption increase up to the relative pressure ca. 0.3 and 0.2, respectively, which can be attributed to the existence of larger micropores and/or small mesopores. In contrast, the adsorption isotherms for ACF-7 and ACF-PAN level off before the relative pressure ca. 0.05 is reached and there is almost no adsorbed volume increase after this point. This indicates that these samples are essentially microporous.

In order to highlight the low-pressure adsorption data, the isotherms are shown in the logarithmic scale in Fig. 2. All samples show a significant nitrogen uptake before relative pressure of 10^{-5} is reached. For ACF-7 and ACF-PAN, the presence of a significant amount of narrow micropores is evident from the fact that about 50% of the total adsorbed amount is achieved below $p/p_0 = 10^{-4}$. This can be ascribed to strong interactions between nitrogen molecules and closely spaced walls of these small pores. Also, for these two samples, a pronounced initial increase in the adsorbed amount and a subsequent more gradual increase is visible, while the adsorption process on ACF-20 and ACF-15 has three distinct stages in the relative pressure ranges of ca. 10^{-7}–10^{-5}, 10^{-5}–10^{-2}, and 10^{-2}–1.0. They can be attrib-

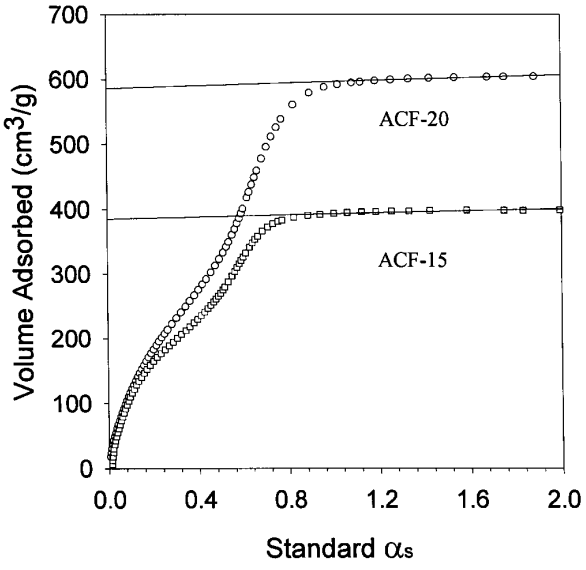

FIG. 4. High-resolution α_s plots for the ACF-20 and ACF-15 activated carbon fibers.

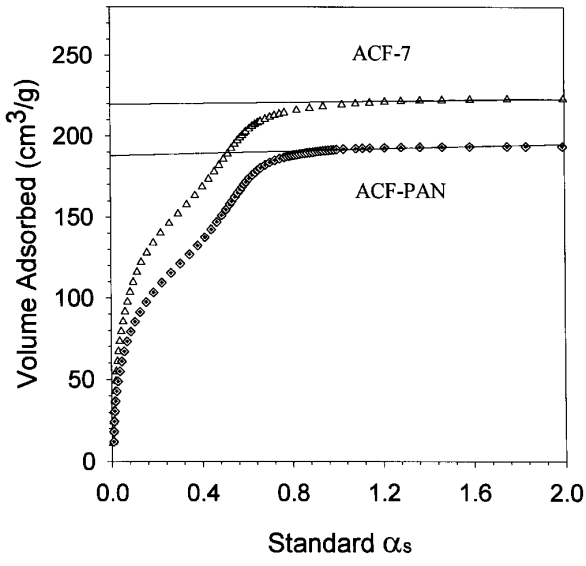

FIG. 5. High-resolution α_s plots for the ACF-7 and ACF-PAN activated carbon fibers.

uted to (i) the filling of small micropores, (ii) the formation of monolayer on the surface of wider micropores and small mesopores as well as the filling of some micropores and increase in the density of the adsorbate in pores which are already filled, and (iii) the condensation inside the larger micropores and small mesopores, respectively. It can be concluded that ACF-15 and ACF-20 have not only micropores but also a significant amount of mesopores.

One of the interesting findings is that ACF-PAN and ACF-7 show similar adsorption patterns in the whole range of relative pressure even though they were made from different precursors. They have similar surface heterogeneity and pore size distributions (see Fig. 3). This may indicate that formation of pores in different types of fibers may be analogous. It was previously reported (36) that narrow micropores are initially formed and after further activation, pores widen and the PSD becomes broader. This can also be seen from the DFT results shown in Fig. 3. The DFT for ACF-20 shows a marked shift in direction to larger pore sizes in comparison to other samples.

2. *Pore Structure Parameters*

High resolution α_s plots of ACFs are shown in Figs. 4 and 5. There are marked filling swings (19, 25, 29) in the low-pressure parts of these plots ($\alpha_s < 0.5$). Also, there are cooperative swings (19, 25, 29) between $0.5 < \alpha_s < 1.0$, showing the existence of larger micropores and/or small mesopores. ACF-15 and ACF-20 exhibit much more pronounced cooperative swing than ACF-7, indicating that they possess significant amounts of larger micropores and/or small mesopores. The point at which the α_s plot begins to show a linearity corresponds to the completion of adsorption in micropores and small mesopores. After this point, a further increase in the amount adsorbed can be attributed to adsorption on the external surface of these adsorbents. All ACF samples show rather low external surface areas and their micropore volumes are very close to the total pore volumes, indicating the presence of very small amounts of macropores or large mesopores. It should be noted that, since some of the ACFs under study exhibit pore size distributions in the size range up to ca. 4 nm (see Fig. 3), the term ''micropore volume'' is used to denote the volume of micropores and small mesopores (up to ca. 4 nm). The BET specific surface area, total pore volume, micropore volume, and external surface area are listed in Table 1.

3. *Pore Size Distributions*

The DFT pore size distributions (PSDs) of ACFs are shown in Fig. 3. They are wider for ACF-20 and ACF-15 than those for ACF-7 and ACF-PAN. The former two samples contain a considerable amount of pores of size between 1.5 and 3.5 nm, while ACF-7 and ACF-PAN have almost no pores larger than 2.0 nm. Because the adsorbed amounts

TABLE 1
Pore Structure Parameters of ACFs

Sample	S_{BET} (m^2/g)	V_{total} (cm^3/g)	V_{micro} (cm^3/g)	$S_{external}$ (m^2/g)
ACF-20	1960	0.94	0.92	10
ACF-15	1430	0.62	0.61	<10
ACF-7	780	0.35	0.34	<10
ACF-PAN	690	0.30	0.30	<10

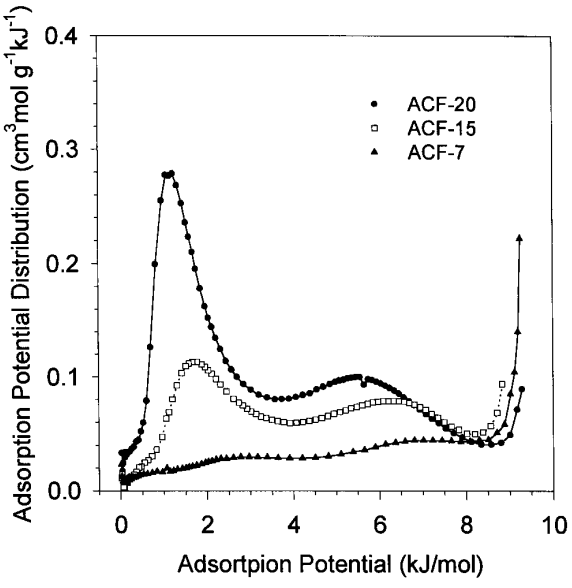

FIG. 6. Adsorption potential distributions for the ACF-20, ACF-15, and ACF-7 activated carbon fibers.

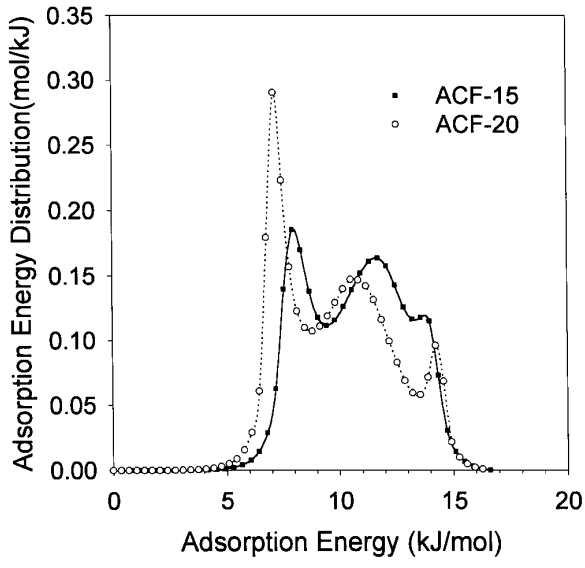

FIG. 7. Adsorption energy distributions for ACF-20 and ACF-15.

at very low pressure ($p/p_0 = 10^{-5}$) are approximately the same for all samples (Fig. 2), pores between 1.5–3.5 nm are the main reason of high surface areas and pore volumes observed for ACF-20 and ACF-15 (Table 1).

4. *Adsorption Potential Distributions*

The adsorption potential distribution $X(A)$ curves are shown in Fig. 6 and clearly indicate the different pore structures of ACFs. All the $X(A)$ functions show two peaks but in the case of the ACF-7, this is less pronounced. An increase in the BET surface area and total pore volume not only causes the shift of the peak positions to lower adsorption potentials, but also changes their relative height. The high adsorption potential values between 8–10 kJ/mol correspond to the micropore filling in small micropores, while the peaks around 5–7 kJ/mol can be attributed mostly to the monolayer formation in the larger micropores and/or mesopores. The peaks around 1–3 kJ/mol result from secondary micropore filling and possibly the multilayer adsorption in wider micropores and mesopores. The obtained results provide a clear evidence for the two-stage filling of supermicropores (pore size above 0.7 nm) and are in agreement with earlier experimental studies of activated carbons (25, 29). One can attempt to find a relationship between the position of peaks on the $X(A)$ distributions and the pore size. However, the positions of the peaks may depend not only on the pore size but also on the pore size distributions and surface properties. A theoretical relationship between the positions of peaks on the adsorption potential distributions and the pore size for homogeneous graphitic slit-like pores has already been reported (24) and can be used in analysis of experimental data, but further studies in this direction are required.

5. *Adsorption Energy Distributions*

The normalized adsorption energy distributions (AEDs) are shown in Figs. 7 and 8. As can be seen, ACFs exhibit broad adsorption energy distributions. The AEDs for all samples show high-energy parts at about 14.0 kJ/mol, which could be correlated to adsorption in narrow micropores. An increase in the BET surface area and pore volume observed in the order from ACF-7 to ACF-15 and to ACF-20 causes a decrease in the fraction of higher energy sites and an

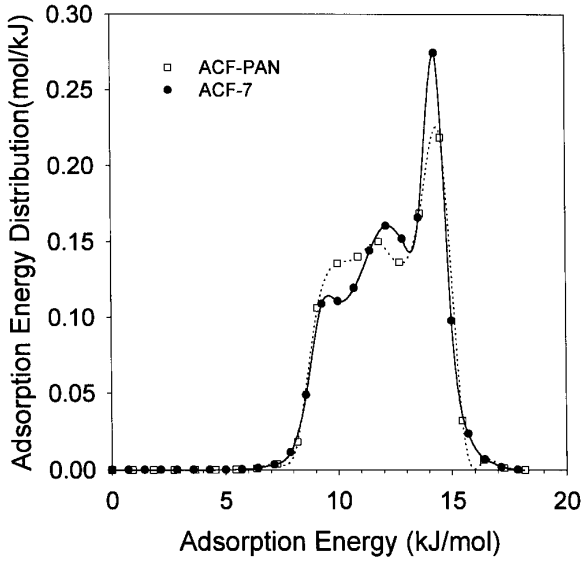

FIG. 8. Adsorption energy distributions for ACF-7 and ACF-PAN.

increase of the low-energy parts, which is accompanied by broadening of the AEDs. Again, the adsorption energy distribution for ACF-PAN is similar to that for ACF-7. Although adsorption energy distributions are model dependent, it is clear that they can provide valuable insight into the properties of activated carbon fibers.

CONCLUSIONS

Nitrogen adsorption isotherms of ACFs were measured in a wide range of relative pressures and the data were analyzed by using the α_s plot and DFT methods as well as adsorption potential distributions and adsorption energy distributions. All samples are microporous, but ACF-15 and ACF-20 exhibit a significant amount of pores on the borderline between the micropore and mesopore size ranges (1.5–3.5 nm). The results revealed that ACFs possess considerable structural and energetic heterogeneity. For ACF-20 and ACF-15, a three-stage adsorption process and corresponding adsorption energy heterogeneity were observed. The DFT software allows us to obtain both micropore and mesopore size distributions which were found in excellent agreement with the results from the α_s plot method and the analysis of adsorption energy distributions and adsorption potential distributions. It is clearly shown that adsorption in supermicropores is a two-stage process and the monolayer formation in these pores takes place at relative pressure range of 10^{-5}–10^{-2}, whereas the condensation inside these pores (possibly preceded by mutilayer formation) takes place between 0.01 and 0.3.

REFERENCES

1. Bansal, R. C., Donnet, J. B., and Stoeckli, F., ''Active Carbon.'' Marcel Dekker, New York, 1988.
2. Jankowska, H., Swiatkowski, A., and Choma, J., ''Active Carbon.'' Ellis Horwood, Chichester, 1991.
3. Suzuki, M., *Carbon* **32,** 577 (1994).
4. Kuwabara, H., Suzuki, T., and Kaneko, K., *J. Chem. Soc., Faraday Trans.* **87,** 1915 (1991).
5. Matsumoto, A., Kaneko, K., and Ramsay, J., *in* ''Fundamentals of Adsorption'' (M. Suzuki, Ed.). Kodansha, Tokyo, 1993.
6. Kaneko, K., and Shiudo, N., *Carbon* **27,** 815 (1989).
7. Matsumoto, A., Ruike, M., Suzuki, T., and Kaneko, K., *Colloids Surf.* **74,** 15 (1993).
8. Matsumoto, A., Tsutsumi, K., and Kaneko, K., *Langmuir* **8,** 2515 (1992).
9. Kaneko, K., Murata, K., Suimizu, K., Camara, S., and Suzuki, T., *Langmuir* **9,** 1165 (1993).
10. Matsumoto, A., and Kaneko, K., *J. Chem. Soc., Faraday Trans. 1* **85,** 3437 (1989).
11. Kaneko, K., *Langmuir* **3,** 357 (1987).
12. Jaroniec, M., Gilpin, R. K., Kaneko, K., and Choma, J., *Langmuir* **7,** 2719 (1991).
13. Kakei, K., Ozeki, S., Suzuki, T., and Kaneko, K., *J. Chem. Soc., Faraday Trans.* **86,** 371 (1991).
14. Lastoskie, C., Gubbins, K. E., and Quirke, N., *J. Phys. Chem.* **97,** 4786 (1993).
15. Dubinin, M. M., and Radushkevich, L. V., *Dokl. Akad. Nauk SSSR* **55,** 327 (1947).
16. Dubinin, M. M., *Prog. Surf. Membr. Sci.* **9,** 1 (1975).
17. Gregg, S. J., and Sing, K. S. W., ''Adsorption, Surface Area and Porosity.'' Academic Press, London, 1982.
18. Rouquerol, J., Avnir, D., Fairbridge, C. W., Everett, D. H., Hayness, J. H., Pernicone, N., Ramsay, J. D. F., Sing, K. S. W., and Unger, K. K., *Pure Appl. Chem.* **66,** 1739 (1994).
19. Jaroniec, M., and Kaneko, K., *Langmuir* **13,** 6589 (1997).
20. Jaroniec, M., and Madey, R., ''Physical Adsorption on Heterogeneous Solids.'' Elsevier, Amsterdam, 1988.
21. Lippens, B. C., and De Boer, J. H., *J. Catal.* **4,** 319 (1965).
22. Mikhail, R., Brunauer, S., and Bodor, E. J., *J. Colloid and Interface Sci.* **24,** 45 (1968).
23. Horvath, G., and Kawazoe, K., *J. Chem. Eng. Jpn.* **16,** 470 (1983).
24. Kruk, M., Jaroniec, M., and Choma, J., *Adsorption* **3,** 209 (1997).
25. Kruk, M., Jaroniec, M., and Gadkaree, K. P., *J. Colloid Interface Sci.* **192,** 250 (1997).
26. Olivier, J. P., *J. Porous Mater.* **2,** 9 (1995).
27. Heuchel, M., Jaroniec, M., Gilpin, R. K., Brauer, P., and Szombathely, M. v., *Langmuir* **9,** 2537 (1993).
28. Lastoskie, C., Gubbins, K. E., and Quirke, N., *Langmuir* **9,** 2693 (1993).
29. Kaneko, K., Ishii, C., Ruike, M., and Kuwabara, H., *Carbon* **30,** 1075 (1992).
30. Sayari, A., Liu, P., Kruk, M., and Jaroniec, M., *Chem. Mater.* **9,** 2499 (1997).
31. Olivier, J. P., Conklin, W. B., and Szombathely, M. v., *in* ''Characterization of Porous Solids III'' (J. Rouquerol, F. Rodrigues-Reinoso, K. S. W. Sing, and K. K. Unger, Eds.), p. 81. Elsevier, Amsterdam, 1994.
32. Mays, T. J., *in* ''Fundamentals of Adsorption'' (M. D. LeVan, Ed.), p. 603. Kluwer, Boston, 1996.
33. Jin, H., Park, S. E., Lee, J. M., and Ryu, S. K., *Carbon* **34,** 429 (1996).
34. Szombathely, M. v., Brauer, M., and Jaroniec, M., *J. Comput. Chem.* **13,** 17 (1992).
35. Kruk, M., Jaroniec, M., and Bereznitski, Y., *J. Colloid Interface Sci.* **182,** 282 (1996).
36. Daley, M. A., Tandon, D., Economy, J., and Hippo, E. J., *Carbon* **34,** 1191 (1996).